Accepted Manuscript

A micro-volume adaptation of a stopped-flow system; use with µg quantities of muscle proteins

J. Walklate, Zoltan Ujfalusi, Vincent Behrens, Edward J. King, Michael A. Geeves

PII: S0003-2697(19)30371-9

DOI: https://doi.org/10.1016/j.ab.2019.06.009

Reference: YABIO 13338

To appear in: *Analytical Biochemistry*

Received Date: 16 April 2019

Revised Date: 7 June 2019

Accepted Date: 10 June 2019

Please cite this article as: J. Walklate, Z. Ujfalusi, V. Behrens, E.J. King, M.A. Geeves, A micro-volume adaptation of a stopped-flow system; use with µg quantities of muscle proteins, *Analytical Biochemistry* (2019), doi: https://doi.org/10.1016/j.ab.2019.06.009.

A micro-volume adaptation of a stopped-flow system; use with µg quantities of muscle proteins

Authors: J Walklate[a], Zoltan Ujfalusi[a,b], Vincent Behrens[c], Edward J King[d] & Michael A Geeves[a]

Addresses:

[a] School of Biosciences, University of Kent, Canterbury, Kent, CT2 7NJ, United Kingdom

[b] Department of Biophysics, University of Pécs, Medical School, Szigeti Street 12, H-7624 Pécs, Hungary

[c] Molecular and Cell Physiology, Hannover Medical School, Germany

[d]TgK Scientific Limited, 7 Long's Yard, St. Margaret's Street, Bradford on Avon, BA15 1DH, United Kingdom

Corresponding author:

Professor Michael Geeves
School of Biosciences
University of Kent
Canterbury CT2 7NJ
UK
M.A.Geeves@kent.ac.uk

Running title: Low volume stopped-flow system

Declaration of interests

EJ King is owner and director of TgK Scientific Ltd., builder and supplier of stopped-flow systems. All other authors have no conflicting interests.

Abstract

Stopped-flow spectroscopy is a powerful method for measuring very fast biological and chemical reactions. The technique however is often limited by the volumes of reactants needed to load the system. Here we present a simple adaptation of commercial stopped-flow system that reduces the volume needed by a factor of 4 to ≈120 µL. After evaluation the volume requirements of the system we show that many standard myosin based assays can be performed using <100 µg of myosin. This adaptation both reduces the volume and therefore mass of protein required and also produces data of similar quality to that produced using the standard set up. The 100 µg of myosin required for these assays is less than that which can be isolated from 100 mg of muscle tissue. With this reduced quantity of myosin, assays using biopsy samples become possible. This will allow assays to be used to assist diagnoses, to examine the effects of post translational modifications on muscle proteins and to test potential therapeutic drugs using patient derived samples.

Key words: rapid mixing, myosin, actin, troponin, myofibrils, Ca regulation, muscle biopsies

Highlights:

- Reduced the volume of sample required in stopped-flow systems by a factor of 4
- Many assays using muscle proteins can be completed with <100 µg of protein
- This is the quantity of protein available from <100 mg of muscle tissues
- This allows assays of human muscle proteins from biopsy tissue

Stopped-flow spectrophotometry is a powerful method for studying chemical and biochemical reactions on msec time scales [1] but often requires relatively large amounts of material. This can be a serious limitation when studying expensive and/or difficult to make samples. There are two major limitations to the sample requirements; the concentration of sample required to give the required signal sensitivity, and the volume of sample required by the equipment. Major advances in sensitivity over recent years have enabled the concentrations of proteins being used to be reduced to sub micromolar, even for a weak signal such as intrinsic tryptophan fluorescence. This allows a greater efficiency of sample usage compared to a few years ago.

In contrast, there has been relatively little change in the volume of sample needed. Typically each shot of the stopped-flow uses at total of 20 µl for a 5 µl observation cell (or 100 µl for a 20 µl observations cell). In a standard single mixing system this volume comes 50:50 from two syringes containing each reactant. Of the order of five shots are normally collected to ensure reproducibility and to allow averaging of the signal to improve the ratio of signal to noise. Thus 50 or 250 µl of each sample are used per data point. However, because of the way the systems are constructed there is a requirement to load between 0.5 to 1 ml of solution in each syringe to prime the system. This is not a problem as a typical experiment can use one filling to complete several measurements. E.g. using a fixed protein concentration mixed with a range of ligand concentrations, or repeating a single measurement at different temperatures. Thus many measurements can be made from a single loading. Other experimental protocols require a new filling for each measurement in which case the total volume required can be excessive for valuable proteins or proteins in limited supply.

We have modified a standard commercial stopped-flow system to include sample loading loops just before the observation chamber. This now allows data to be collected using a single loading of 120 µl of each sample with no loss of sensitivity. This represents a 4-8 fold reduction in the volume of sample needed to complete a typical measurement. For example it is now possible to complete a

measurement of the affinity of actin for myosin using ≈1 µg of the 42 kDa protein, actin (5 x 120 µL of a 30 nM sample).

Here we describe the modification which, in principle, can be made to most commercial stopped-flow systems, and demonstrate its utility for a variety of reactions using the muscle proteins actin, myosin, tropomyosin and the troponin complex (TnT, TnC and TnI). The quantities of protein required are those which would be available for myosin isolated from a 100 mg human biopsy sample opening up a range of possible diagnostic applications.

Methods:

Design of the micro-volume system.

The modification of the stopped-flow system is similar to that we reported previously to allow much wider range of temperature control of the stopped-flow [2]. A small module was constructed from PEEK containing flow lines, two 3-way valves and a set of 3 PTFE compression fittings (on the front and rear face) to match those on the face of the stopped-flow drive unit and the mixing/observation unit. The unit was inserted between the stopped-flow drive unit and the mixing/observation chamber as illustrated in Fig 1. The system flow circuit is illustrated in Fig 1A, while Fig 1B & 1C are photographs of the stopped-flow drive unit and micro-volume unit. The micro-volume module design allowed approximately 120 µl of sample to be drawn into the loading loops leading to the mixing/observation chamber. Buffer from the standard drive syringes was then used to drive the sample from the loading loops through the mixing unit into the observation chamber. Since the overall configuration of the system has not changed the overall performance of the equipment in terms of dead-time (the age of the sample on arrival in the observation chamber), and optical sensitivity was not expected or found to be altered.

In a typical experiment 150 µl was pipetted into the conical loading cup avoiding air bubbles. With the valve in the position to connect the loading cup to the observation cell, the stop syringe was used to draw 120 µl of sample into the loading line, and the valve was then switched to connect the drive syringe through loading loop to the observation cell. The procedure could be repeated for the second sample loop if required. Using a 5 µl observation cell a series of 20 µl shots (10 µl from each drive syringe) were collected. Continuing to drive multiple shots will rinse the loading loops and cell and leave system primed with buffer ready for the next sample loading.

Proteins

Myosin subfragment 1 (S1) was obtained by extracting myosin from Rabbit psoas muscle [3] and digested with α-chymotrypsin [4]. A Sepharose FF column was used to purify the S1 which was freeze-dried in a 5 mM potassium phosphate buffer with 1% sucrose and stored at -80 °C. S1 powder was dissolved in experimental buffer and dialysed overnight to remove the sucrose and phosphate. The protein concentration was determined by absorbance at 280 nm ($\varepsilon^{1\%}$ = 7.9 cm^{-1}, MW = 115 kDa) using a Varian Cary 50 Bio UV spectrophotometer.

Actin was prepared from rabbit skeletal muscle [5]. Actin was labelled at cysteine-374 with pyrene for use in stopped-flow experiments with an average label content of ≈90% determined by protein and pyrene absorbance previously described [6].

Tropomyosin and troponin was purified during the actin purification using methods previously described [7,8].

Myofibrils were prepared as previously described [9,10] with some modifications. Briefly mouse *Gastrocnemius* muscle strips equilibrated in fiber preparation buffer containing: 6 mM Imidazole, 8 mM Mg-Acetate, 70 mM Propionate pH 7.0, 5 mM EGTA, 7 mM ATP, 1 mM NaN_3. The buffer was exchanged twice before being left to permeabilize for 2 hours in fiber preparation buffer containing 0.5 % Triton X-100. For storage, fibers were equilibrated in fiber prep buffer containing 50 % glycerol

and kept at -20 °C until needed. To obtain myofibrils 60-100 mg of fibers were homogenised using an electric homogeniser (Dremel cordless moto-tool model 850) for 15 seconds at low speed (15,000 rpm) and left to cool on ice for >1 minute. This was repeated 3-4 times. Myofibril integrity was checked using a light microscope, if large bundles of myofibrils were present then further homogenisation was performed to help break them up to individual myofibrils. Fibers were homogenised in a *rigor*-buffer containing: 50 mM Imidazole, 12 mM Mg-Acetate, 2 mM EGTA, and 106 mM NaCl pH 7.0. Myofibril stopped-flow assays were conducted with 2'/3'-O-(N-Methyl-anthranoloyl)-ATP (mantATP, Jenna Bioscience). Muscle tissue was collected in accordance with the U.K. Animals (Scientific Procedures) Act 1986 and associated guidelines.

Results

Test of the system

To test the micro-volume system we compared the transients observed for a standard reaction using the stopped-flow system in normal mode with those using the micro-volume unit (MVU). Due to the MVU being added between the drive syringes and the observation cell the dead time was investigated to see if this was affected. Here a 0.5 µM complex of pyrene labelled actin and myosin subfragment 1 (pyr-A.S1) was dissociated by addition of 10 µM to 2 mM MgATP. The reaction was observed as a large increase in pyrene fluorescence (F) as the S1.ATP dissociated from the pyr-A. The acto.S1 was loaded into the system via the MVU while the ATP was loaded using the standard method so that one syringe contained buffer and the other ATP. Figure 2A shows the transients using 10 µM and 2 mM MgATP with both the standard and MVU setups. The averaged transients shown demonstrate that the signal-to-noise of the standard and MVU are comparable as expected since the optical cell is identical in both cases. Small differences changes in fluorescence baseline are attributed to the time taken switch between experimental setups. As the MgATP concentration was increased from 10 µM to 2 mM the k_{obs} also increased, this results in a loss of fluorescence amplitude in the dead time of the machine (time between mixing and measurement recording). A

plot of the ln(ΔFl) versus the k_{obs} (Figure 2B) was linear and the slope defines the dead time of the stopped-flow machine. For the standard setup this was 0.64 ± 0.08 ms and for the MVU this was 0.56 ± 0.08 ms and therefore very similar and compared with the manufactures estimate of 0.7 ms. This is to be expected because the observation cell volume and shot volumes and flow speeds do not change between the two methods.

To investigate the number of usable transients different volumes of 0.5 µM pyr-A.S1 were loaded and mixed against 10 µM MgATP with 20 shots measured to observe the washout of the sample. Figure 3A illustrates a selection of transients collected using the MVU with a 120 µL loading volume and using 20 µl shots (10 µl from each syringe) and a 5 µl observation cell. Each transient could be well described by a single exponential function $F_t = F_o \cdot \exp(-k_{obs} \cdot t)$ where k_{obs} is the pseudo first order rate constant for ATP binding to pyr-A.S1. From the first shot (not shown) the observed amplitude of the transient was large (~40%) and relatively consistent over the first 6 shots (60 µl from each syringe) and then decayed rapidly such that by shot 10 the amplitude was only a quarter of the starting value. This decline in amplitude represents the wash out of the sample. Figure 3B plots the relative amplitude (observed amplitude/end point to correct for small differences between total intensity) against shot number and compares it with that of the same solution using the standard stopped-flow set up (filled squares). Three loading volumes (80 µl – open squares, 100 µl – closed triangles and 120 µl – open triangles) were investigated to determine the minimum loading volume that could be used and still obtain similar traces to that seen with the standard set up. While the 80 and 100 µl load volumes did give similar traces to that seen with the standard method, the initial shots increased in relative fluorescence amplitude to that seen with the standard method before washing out as seen with the 120 µl load volume. This was attributed to the load volume not being sufficient to completely fill the sample lines from the loading cup to the observation cell, therefore there was dilution of the sample in the first few shots with the buffer proceeding it. With the 120 µl load volume however, compared with the standard set up, the two are very similar for shots 1-7.

Note that the best fit k_{obs} values (24.2 ± 0.3 s^{-1}) were independent of shot number over the range 1 – 11 indicating the correct k_{obs} could be estimated even for very low amplitudes. This is because the k_{obs} is independent of protein concentration but linearly dependent upon ATP concentration. ATP was maintained constant as we did not use the loading loop for this reagent.

The pyrene actin signal is very strong with a large signal change. The same test was therefore repeated with a much weaker tryptophan fluorescence signal (Figure 4). In the absence of actin, ATP binds to S1 with a 12-15 % increase in fluorescence. 10 µM ATP was rapidly mixed with 0.5 µM S1 and the tryptophan signal recorded. As before a 120 µL sample was loaded into one loading loop and a series of 20 µL shots collected. ATP was loaded using the standard set up so that one syringe contained buffer and the other contained ATP. Figure 4A illustrates how the signal was both much weaker and with a smaller amplitude compared to pyrene-actin, but the number of useful shots is very similar (shots 1-7). The amplitude is reasonably constant for shots 1-7 with a 120 µl loading volume then begins to decrease sharply after shot 7 returning to baseline by shot 13 (Figure 4B). The weaker, noisy signal gives more variation in the fitted value of k_{obs} (22.8 ± 0.7 s^{-1}) but within the limits of the noise. As with the pyrene-labelled actin a 120 µl load volume gave the most consistent traces over the most number of shots before the sample began to wash out.

K_D measurements

Having determined an appropriate loading volume of 120 µl that allowed us to obtain consistent traces over a limited number of shots, we then investigated whether we could perform a series of assays and obtain data similar to the standard setup. A method developed by Kurzawa and Geeves [11] for determining the actin affinity of S1 relies on monitoring the relative fluorescence amplitude as a varied concentration of S1 is pre-incubated with a fixed (30 nM) concentration of actin and rapidly mixed with a fixed (20 µM) concentration of ATP. As the S1 concentration was increased the relative fluorescence amplitude also increased as more of the pyrene labels that were initially quenched by the bound S1 are revealed upon ATP-induced dissociation. This assay uses a large

amount of protein with µM amounts of S1 being needed in some cases. This assay then lends itself very well to testing the applications of the micro-volume unit.

Figure 5A shows example traces of 30 nM pyrene labelled actin pre-incubated with varied concentrations of S1 then rapidly mixed with 20 µM MgATP in the stopped-flow. The pyrene labelled actin.S1 was loaded into the micro-volume unit while the MgATP was loaded via the standard method of the drive syringes. The relative fluorescence amplitudes could then be plotted against the S1 concentration which was best described by a quadratic equation (Eq 1, Figure 5B).

$$\propto = \frac{[M] + K_D + [A]_0 - \sqrt{([M] + K_D + [A]_0)^2 - \frac{4}{[M][A]_0}}}{2[A]_0} \qquad Eq\ 1$$

Figure 5B shows triplicate repeats of this assay to highlight the reproducibility of the data obtained by the micro-volume unit. The average K_D value from the three repeats was 45.5 ± 2.6 nM which is in good agreement with the findings of Kurzawa and Geeves which was 44 nM [11].

pCa measurements

A second assay that requires a large amount of protein is the calcium sensitivity assay where actin is complexed with the thin-filament calcium-regulatory proteins [12] – tropomyosin and troponin. The assay is conducted in a series of Ca-EGTA buffers containing increasing concentrations of free calcium and therefore requires a different solution filling both syringes of the stopped-flow for each new calcium concentration. In this assay a solution of myosin S1 was mixed with a 10 fold excess of actin·TmTn at different free calcium concentration (Fig 5 A & B). At high calcium concentrations all the actin sites are available and a single exponential was observed as S1 binds to 1 in 10 of the available sites (pseudo first order in [actin]). Here $k_{obs} = [actin]k_{+1}$ where k_{+1} is the 2nd order rate constant for S1 binding to actin. As calcium concentration is reduced the TmTn complex blocks access to a fraction of the actin sites reducing the effective concentration of available actin. In this case $k_{obs} = [actin]k_{+1} \cdot K_B/(1 + K_B)$ and $K_B = [A_{blocked}]/[A_{available}]$. A plot of k_{obs} vs calcium concentration gives the calcium dependence of K_B.

The same experiment can be repeated but reversing the two protein concentrations; mixing a ten-fold excess of myosin S1 with actin·TmTn. This approach uses much less actin·TmTn but conversely more myosin S1. The reaction is also more complex to analyse because as S1 binds to actin·TmTn at low calcium concentration it displaces TmTn from actin making more actin sites available thus accelerating the binding reaction. Fig 5 C illustrates how the reaction changed from an exponential to sigmoid binding transient as calcium concentration was reduced. Full analysis of the reaction is complex [13] but a simple plot of half-times for the transient (Fig 5D) yielded a similar plot to that of Fig 5B.

Myofibrils

Myofibrils (muscle cell fragments a few 10's of µm long containing the intact sarcomeres) are an important way of measuring muscle mechanics of an organised system [14–16]. Some biochemical kinetic studies have used rapid mixing systems with myofibrils [17,18] combined with either intrinsic tryptophan fluorescence or pyrene labelling of actin [18]. A limitation of using the tryptophan fluorescence is that high concentrations (3 µM) were needed. Labelling the myofibrils with pyrene could be a reasonable alternative but due to indiscriminate binding there is no guarantee that only cysteine-374 of actin would be labelled [17,18]. Here we have used mantATP, a fluorescently labelled ATP analogue, which increases in fluorescence when bound to myosin [17,19]. Figure 7A shows example traces of 200 nM Mouse *Gastrocnemius* myofibrils rapidly mixed with varied mantATP concentrations using the micro-volume unit. These traces using both the standard setup and MVU were best described by a double exponential, with the fast phase associated with the mantATP binding and the second phase of unknown origin. Previous work using S1 and mantdATP showed that two phases were present when only one isomer of mantATP was used [20]. When looking at tryptophan fluorescence Stehle et al also witnessed this slow phase and attributed it to the ATP hydrolysis step [18]. For our purposes we have focused on the fast phase as this the mantATP binding step which is known to be dependant of ATP concentration. Due to mantATP being

fluorescently tagged, as the concentration of mantATP increases so does the background fluorescence signal and therefore at high mantATP concentrations the signal change associated with binding is lost in the noise. We were unable to perform a full ATP binding assay because of this, however we were able to determine the K_1k_{+2} value over a smaller mantATP concentration (1-5 μM mantATP). When the k_{obs} is plotted against the mantATP concentration (figure 7B) there is a linear dependence which from the slope gives the K_1k_{+2}. Figure 7B shows the averages for the standard setup (black squares) and the MVU setup (empty squares) which are in good agreement with each other: 1.76 μM ± 0.07 μM^{-1} s^{-1} and 1.92 ± 0.03 μM^{-1} s^{-1} respectively.

Discussion

Summary of performance

We have described here assays that rely on measuring the change in fluorescence, and changes in the observed rate constant using the MVU with results comparable with published data using the standard stopped-flow setup. Once accustomed to the method of loading samples on the stopped-flow using the MVU, the process is the same as the standard setup. The same caution should be taken as with the standard setup to avoid as best as possible air bubbles from entering the system.

Mass of protein used in each assay

Reducing the volume of the samples loaded onto the stopped-flow in combination with the low concentrations being used means the mass of protein in each assay is now reduced at least 4 fold compared the standard system . Table 1 shows the estimated quantity of protein used in each of the assays presented here compared to using the standard setup. The calculations assume the MVU uses 120 μl samples per data point. As listed in Table 1 the quantities of S1 need for the assays of figure 5 & 6 are < 50 μg in each case. Note that actin, tropomyosin and troponin are not usually in limited supply. These quantities of S1 (< 50 μg) compare favourably with the 500 μg of active S1 that can be

purified from ~ 100 mg of mammalian muscle tissue or the 100-225 µg from the indirect flight muscle of 170-250 Drosophila [21].

To perform the full set of assays to characterise the kinetics of a myosin such as we have done with recombinantly expressed human S1, [22–26] and based on 1 mg/ml of S1 ≈ 8 µM and that 0.12 ml was used for the collection of each data point, the total amount of required is 0.3 mg.

Potential uses

Stopped-flow is a very powerful tool for teasing apart the fast kinetic steps (millisecond time scale) of chemical and biochemical reactions. One limiting factor has always been the amount of sample needed to perform measurements. Improved sensitivity of the equipment and more potent fluorophores have helped to reduce the concentrations needed in experiment. Using the micro-volume method presented here improves the economy of sample usage even further and now will allow studies not previously possible with a reduction in protein used by at least 1/4 (see above).

Our interest is in muscle proteins, in particular myosins where large quantities of protein are often not available. Tissue purified protein often contains a mixture of isoforms and so complicates the interpretation of data. Single mammalian muscle fibers normally contain a single isoform [27] and purification of myosin from single muscle fibers (typically 0.1 x 10-20 mm) can yield ≈2 µg of myosin in 50 µl [28].

Conventional expression systems using *E. coli* and Baculovirus are not applicable for recombinant myosin expression due to a lack of appropriate chaperones [29–33]. Recombinant human myosin motor domains have been successfully produced using a mouse C2C12 cell system [34] and from this characterisation of 7 of the 8 skeletal and cardiac myosin isoforms have been completed along with mutations in the myosin that lead to myopathies [22–26,34,35]. A drawback to this method of recombinant myosin production is a large cost (growing viruses and then transfecting and growing

mammalian cells) and obtaining small quantities of motor domain (≈1-2 mg). By using the method presented here it will be possible to perform more assays with the limited amount of protein.

Failing a recombinant expression system the only alternative source of muscle myosin is from muscle tissue. Samples of this type bring up moral and ethical issues and as scientists we should abide by the 3 R's (Replace, Reduce, and Refine). Human muscle biopsies come from two sources needle biopsies from volunteers and samples from tissue banks often holding samples from human cardiac tissue obtained either from donor hearts not used in transplants or from cardiac septal myectomies. Such samples are very small ≈100 mg. Such tissue samples will now prove useful for either protein or myofibril studies. An advantage of using biopsy samples over recombinantly expressed proteins is that in muscle myopathies myosin can carry a range of post translational modification and individuals are usually heterozygous for the mutations. Being able to use biopsy tissue will allow us to test how a mixture of wild type and mutant proteins behave.

Myofibrils

This modification is a simple and effective method of reducing the volume of sample required to perform stopped-flow assays whilst maintaining the accuracy of the standard set up of the machine. This could allow researchers with limited samples to be able to use this method in an efficient manner saving them both time and money.

Acknowledgements

This work was supported by EU Horizon 2020 grant SILICO-FCM 777204 and the British Heart Foundation grant No 30200. Sam Lynn for purification of myosin S1 and actin.

[1] X. Zheng, C. Bi, Z. Li, M. Podariu, D.S. Hage, Analytical methods for kinetic studies of biological interactions: A review., J. Pharm. Biomed. Anal. 113 (2015) 163–80. doi:10.1016/j.jpba.2015.01.042.

[2] J. Walklate, M.A. Geeves, Temperature manifold for a stopped-flow machine to allow measurements from -10 to +40 °c, Anal. Biochem. 476 (2015). doi:10.1016/j.ab.2015.01.020.

[3] S.S. Margossian, S. Lowey, Preparation of myosin and its subfragments from rabbit skeletal muscle., Methods Enzymol. 85 Pt B (1982) 55–71.

[4] A.G. WEEDS, R.S. TAYLOR, Separation of subfragment-1 isoenzymes from rabbit skeletal muscle myosin, Nature. 257 (1975) 54–56. doi:10.1038/257054a0.

[5] J.A. Spudich, S. Watt, The regulation of rabbit skeletal muscle contraction. I. Biochemical studies of the interaction of the tropomyosin-troponin complex with actin and the proteolytic fragments of myosin., J. Biol. Chem. 246 (1971) 4866–71.

[6] A.H. Criddle, M.A. Geeves, T. Jeffries, The use of actin labelled with N-(1-pyrenyl)iodoacetamide to study the interaction of actin with myosin subfragments and troponin/tropomyosin., Biochem. J. 232 (1985) 343–9.

[7] M.L. Greaser, J. Gergely, Reconstitution of troponin activity from three protein components., J. Biol. Chem. 246 (1971) 4226–33.

[8] S. Ebashi, T. Wakabayashi, F. Ebashi, Troponin and its components., J. Biochem. 69 (1971) 441–5.

[9] P.J. Knight, J.A. Trinick, Preparation of myofibrils., Methods Enzymol. 85 Pt B (1982) 9–12.

[10] C. Herrmann, J. Sleep, P. Chaussepied, F. Travers, T. Barman, A structural and kinetic study on myofibrils prevented from shortening by chemical cross-linking, Biochemistry. 32 (1993) 7255–7263. doi:10.1021/bi00079a023.

[11] S.E. Kurzawa, M.A. Geeves, A novel stopped-flow method for measuring the affinity of actin for myosin head fragments using ?g quantities of protein, J. Muscle Res. Cell Motil. 17 (1996) 669–676. doi:10.1007/BF00154061.

[12] S.E. Boussouf, R. Maytum, K. Jaquet, M.A. Geeves, Role of tropomyosin isoforms in the calcium sensitivity of striated muscle thin filaments, J. Muscle Res. Cell Motil. 28 (2007) 49–58. doi:10.1007/s10974-007-9103-z.

[13] S.M. Mijailovich, X. Li, R.H. Griffiths, M.A. Geeves, The Hill model for binding myosin S1 to regulated actin is not equivalent to the McKillop-Geeves model., J. Mol. Biol. 417 (2012) 112–28. doi:10.1016/j.jmb.2012.01.011.

[14] A. Belus, N. Piroddi, B. Scellini, C. Tesi, G.D. Amati, F. Girolami, M. Yacoub, F. Cecchi, I. Olivotto, C. Poggesi, The familial hypertrophic cardiomyopathy-associated myosin mutation R403Q accelerates tension generation and relaxation of human cardiac myofibrils, J. Physiol. 586 (2008) 3639–3644. doi:10.1113/jphysiol.2008.155952.

[15] N. Piroddi, A. Belus, B. Scellini, C. Tesi, G. Giunti, E. Cerbai, A. Mugelli, C. Poggesi, Tension generation and relaxation in single myofibrils from human atrial and ventricular myocardium, Pflügers Arch. - Eur. J. Physiol. 454 (2007) 63–73. doi:10.1007/s00424-006-0181-3.

[16] P.P. de Tombe, A. Belus, N. Piroddi, B. Scellini, J.S. Walker, A.F. Martin, C. Tesi, C. Poggesi, Myofilament calcium sensitivity does not affect cross-bridge activation-relaxation kinetics, Am. J. Physiol. Integr. Comp. Physiol. 292 (2007) R1129–R1136. doi:10.1152/ajpregu.00630.2006.

[17] Y.Z. Ma, E.W. Taylor, Kinetic mechanism of myofibril ATPase, Biophys. J. 66 (1994) 1542–1553. doi:10.1016/S0006-3495(94)80945-2.

[18] R. Stehle, C. Lionne, F. Travers, T. Barman, Kinetics of the Initial Steps of Rabbit Psoas Myofibrillar ATPases Studied by Tryptophan and Pyrene Fluorescence Stopped-Flow and

Rapid Flow-Quench. Evidence That Cross-Bridge Detachment Is Slower than ATP Binding †, Biochemistry. 39 (2000) 7508–7520. doi:10.1021/bi0004753.

[19] K.H. Myburgh, K. Franks-Skiba, R. Cooke, Nucleotide turnover rate measured in fully relaxed rabbit skeletal muscle myofibrils., J. Gen. Physiol. 106 (1995) 957–73.

[20] S.K.A. Woodward, J.F. Eccleston, M.A. Geeves, Kinetics of the interaction of 2'(3')-O-(N-methylanthraniloyl)-ATP with myosin subfragment 1 and actomyosin subfragment 1: Characterization of two acto.cntdot.S1.cntdot.ADP complexes, Biochemistry. 30 (1991) 422–430. doi:10.1021/bi00216a017.

[21] M.J. Bloemink, C.M. Dambacher, A.F. Knowles, G.C. Melkani, M.A. Geeves, S.I. Bernstein, Alternative exon 9-encoded relay domains affect more than one communication pathway in the Drosophila myosin head., J. Mol. Biol. 389 (2009) 707–21. doi:10.1016/j.jmb.2009.04.036.

[22] J.C. Deacon, M.J. Bloemink, H. Rezavandi, M.A. Geeves, L.A. Leinwand, Erratum to: Identification of functional differences between recombinant human α and β cardiac myosin motors., Cell. Mol. Life Sci. 69 (2012) 4239–55. doi:10.1007/s00018-012-1111-5.

[23] M.J. Bloemink, J.C. Deacon, D.I. Resnicow, L.A. Leinwand, M.A. Geeves, The superfast human extraocular myosin is kinetically distinct from the fast skeletal IIa, IIb, and IId isoforms., J. Biol. Chem. 288 (2013) 27469–79. doi:10.1074/jbc.M113.488130.

[24] M. Bloemink, J. Deacon, S. Langer, C. Vera, A. Combs, L. Leinwand, M.A. Geeves, The hypertrophic cardiomyopathy myosin mutation R453C alters ATP binding and hydrolysis of human cardiac β-myosin., J. Biol. Chem. 289 (2014) 5158–67. doi:10.1074/jbc.M113.511204.

[25] S. Nag, R.F. Sommese, Z. Ujfalusi, A. Combs, S. Langer, S. Sutton, L.A. Leinwand, M.A. Geeves, K.M. Ruppel, J.A. Spudich, Contractility parameters of human β-cardiac myosin with the hypertrophic cardiomyopathy mutation R403Q show loss of motor function., Sci. Adv. 1 (2015) e1500511. doi:10.1126/sciadv.1500511.

[26] J. Walklate, C. Vera, M.J. Bloemink, M.A. Geeves, L. Leinwand, The most prevalent freeman-sheldon syndrome mutations in the embryonic myosin motor share functional defects, J. Biol. Chem. 291 (2016). doi:10.1074/jbc.M115.707489.

[27] M.A. Pellegrino, M. Canepari, R. Rossi, G. D'Antona, C. Reggiani, R. Bottinelli, Orthologous myosin isoforms and scaling of shortening velocity with body size in mouse, rat, rabbit and human muscles., J. Physiol. 546 (2003) 677–89.

[28] S. Weiss, R. Rossi, M.-A. Pellegrino, R. Bottinelli, M.A. Geeves, Differing ADP Release Rates from Myosin Heavy Chain Isoforms Define the Shortening Velocity of Skeletal Muscle Fibers* Downloaded from, J. Biol. Chem. 276 (2001) 45902–45908. doi:10.1074/jbc.M107434200.

[29] J.M. Barral, A.H. Hutagalung, A. Brinker, F.U. Hartl, H.F. Epstein, Role of the Myosin Assembly Protein UNC-45 as a Molecular Chaperone for Myosin, Science (80-.). 295 (2002) 669–671. doi:10.1126/science.1066648.

[30] D. Chow, R. Srikakulam, Y. Chen, D.A. Winkelmann, Folding of the Striated Muscle Myosin Motor Domain, J. Biol. Chem. 277 (2002) 36799–36807. doi:10.1074/jbc.M204101200.

[31] M.G. Price, M.L. Landsverk, J.M. Barral, H.F. Epstein, Two mammalian UNC-45 isoforms are related to distinct cytoskeletal and muscle-specific functions., J. Cell Sci. 115 (2002) 4013–23.

[32] R. Srikakulam, D.A. Winkelmann, Myosin II folding is mediated by a molecular chaperonin., J. Biol. Chem. 274 (1999) 27265–73.

[33] R. Srikakulam, D.A. Winkelmann, Chaperone-mediated folding and assembly of myosin in striated muscle., J. Cell Sci. 117 (2004) 641–52. doi:10.1242/jcs.00899.

[34] D.I. Resnicow, J.C. Deacon, H.M. Warrick, J.A. Spudich, L.A. Leinwand, Functional diversity among a family of human skeletal muscle myosin motors., Proc. Natl. Acad. Sci. U. S. A. 107 (2010) 1053–8. doi:10.1073/pnas.0913527107.

[35] Z. Ujfalusi, C.D. Vera, S.M. Mijailovich, M. Svicevic, E.C. Yu, M. Kawana, K.M. Ruppel, J.A. Spudich, M.A. Geeves, L.A. Leinwand, Dilated cardiomyopathy myosin mutants have reduced force-generating capacity, J. Biol. Chem. 293 (2018) 9017–9029. doi:10.1074/jbc.RA118.001938.

Figure 1

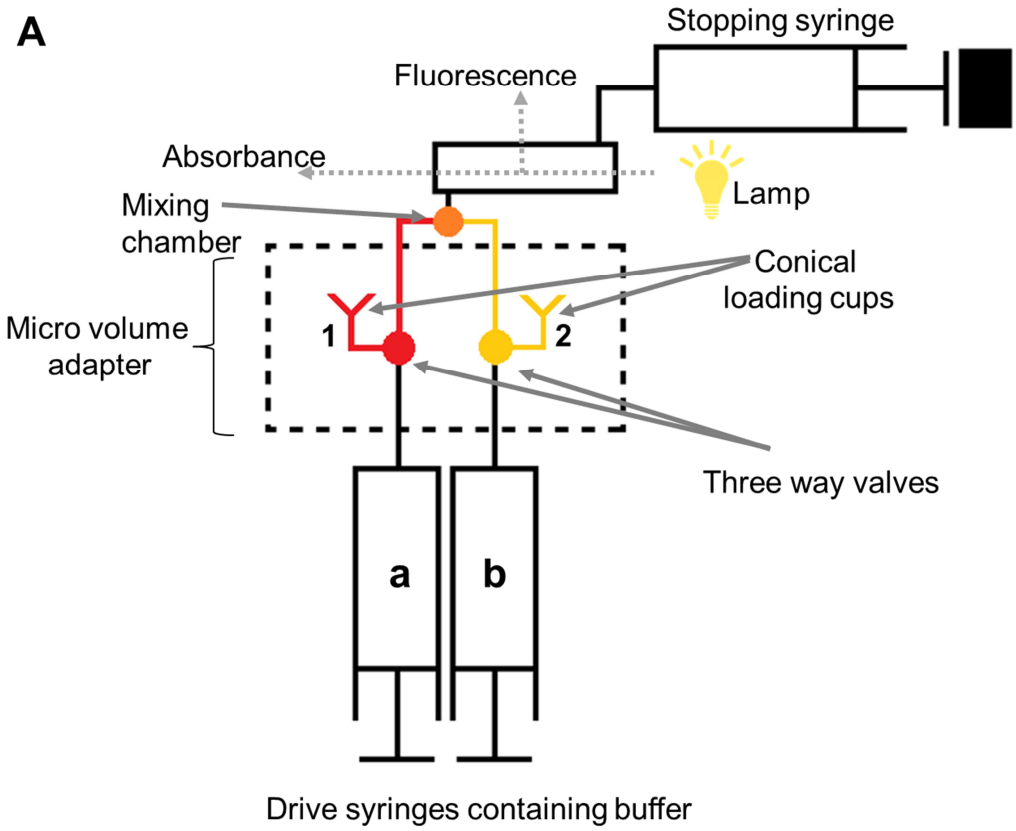

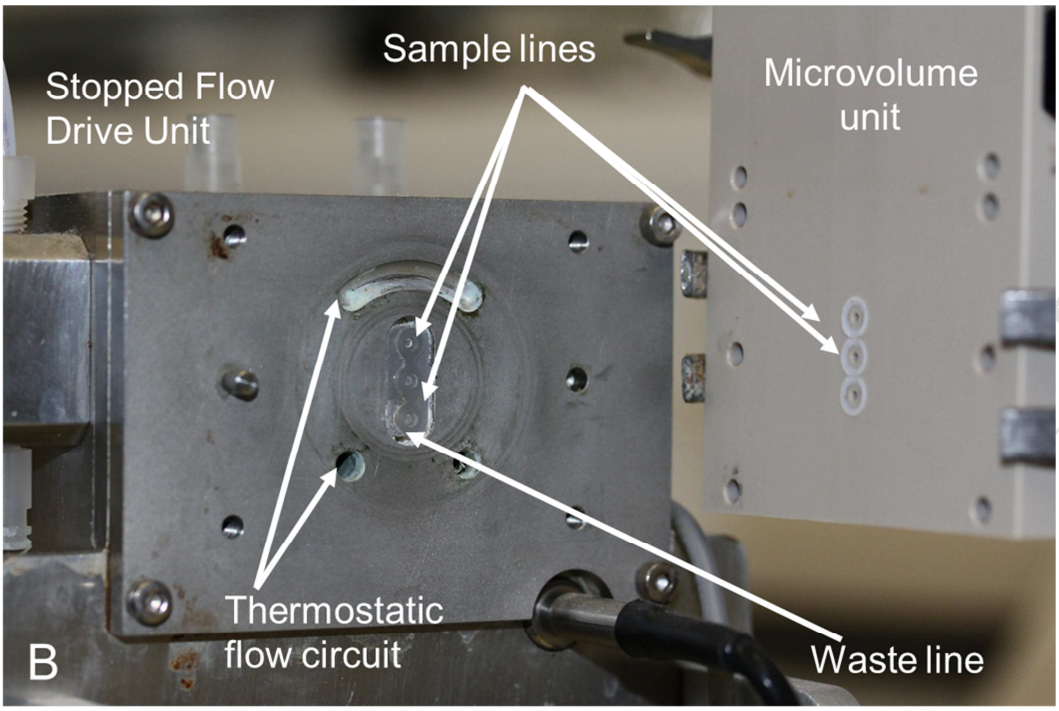

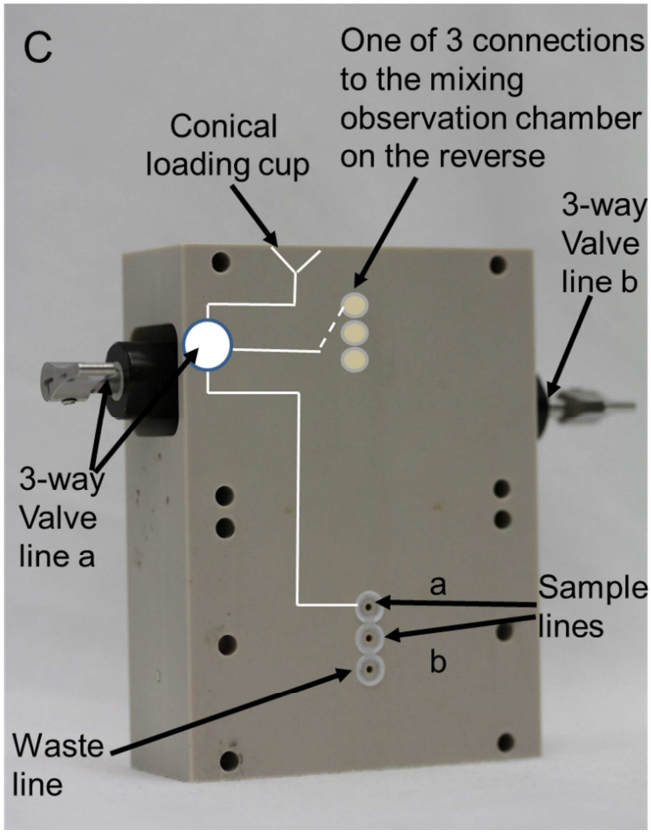

Figure 1. (A) Diagram of the micro-volume unit attached to the stopped-flow system. The micro-volume unit sits between the drive syringes and the mixing chamber of a standard stopped-flow system. Samples can be loaded individually into the conical cups. Three way valves allow the sample

to be drawn into the sample tubes between the valves and the mixing chamber using the stopping syringe. Switching the valves connects the drives syringes (containing buffer) to the mixing chamber. Approximately 7 x 20 µl shots (10 µl from each of lines a & b) can be collected reproducibly – see Results. (B) Photo of the rear of the stopped-flow drive unit showing the matching face of the micro-volume unit. (C) Photo of the rear of the micro-volume unit. The filling/drive lines for one of the three lines (sample a, b and the waste) is indicated in white. Only one line is drawn as the circuit is complex in 3D. The mixing/observation assembly affixes to the other face of the unit via an identical set of 3 compression fittings.

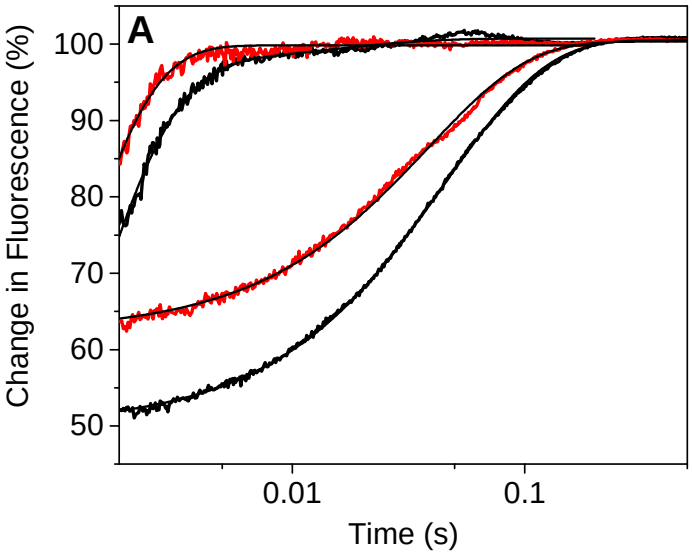

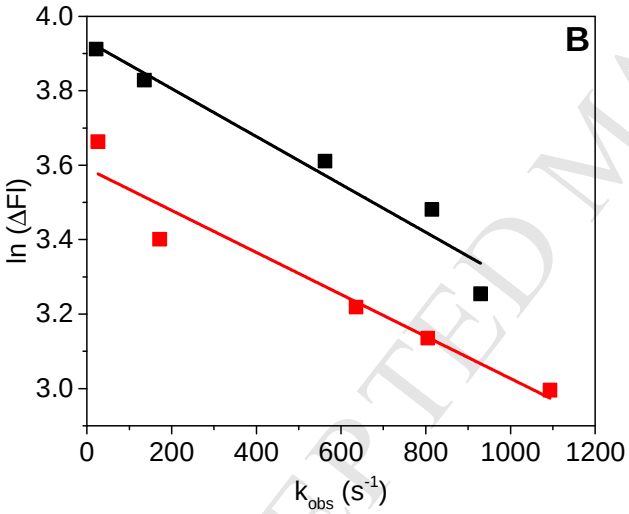

Figure 2: Dead time calibration of the MVU compared to the standard setup using Rabbit pyrene-labelled actin.S1 (pyr-A.S1) rapidly mixed with MgATP. (A) 0.5 µM pA.S1 was rapidly mixed with either 10 µM or 2 mM MgATP using the standard set (black lines) up or the MVU (red lines). As the concentration of MgATP increases so does the observed rate constant (k_{obs}). These were best described by a single exponential. (B) A plot of the ln(change in fluorescence) versus the k_{obs} results in a linear dependence, the slope of which gives the dead time of the machine. For the standard setup (black) the dead time = 0.64 ± 0.08 ms and for the MVU (red) the dead time = 0.56 ± 0.08 ms.

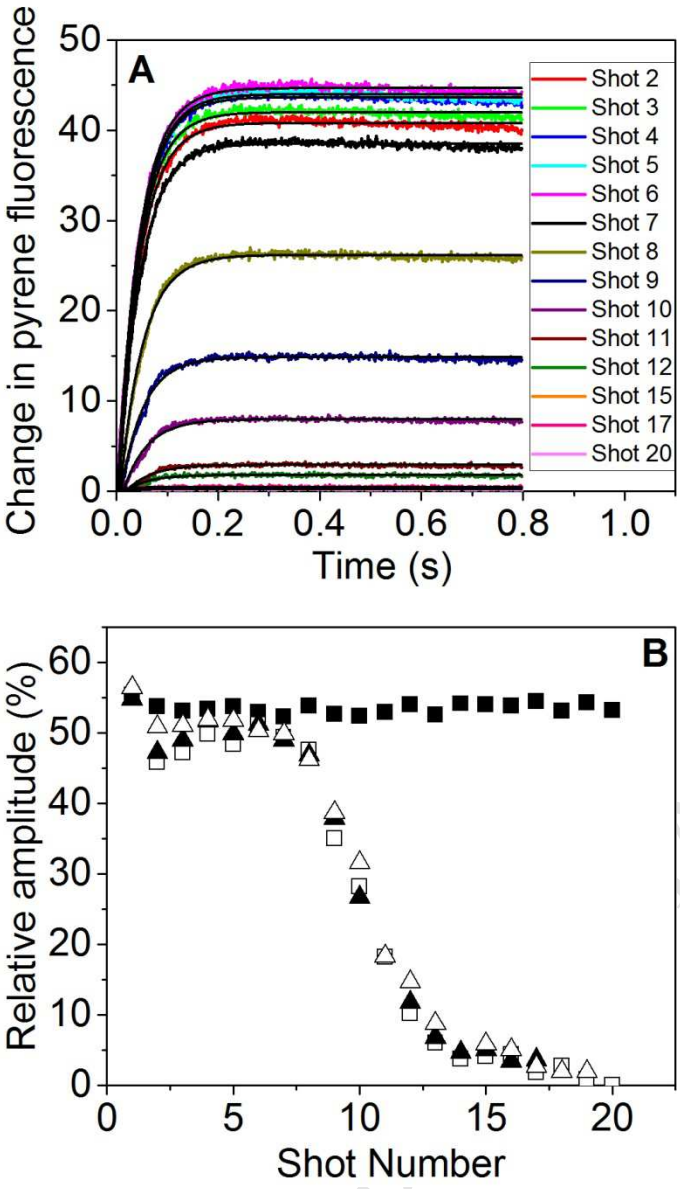

Figure 3: ATP induced dissociation of pyrA.S1 by ATP. 20 µM ATP was loaded into one drive syringe as per the standard stopped-flow method while buffer was loaded into the other drive syringe. 120 µL of 1 µM pyrA.S1 was loaded into the loading loop of the MVU before 20 'shots' were collected. (A) A selection of the 20 transients are displayed to show that the protein is present at a high concentration in the first 6-7 shots. The change in fluorescence decreasing shows the acto.S1 washing out of the system and buffer is replacing it. (B) The relative fluorescence amplitude for the standard method (closed squares) versus MVU using

a loading volume of 80 µl (open squares), 100 µl (closed triangles) and 120 µl (open triangles).

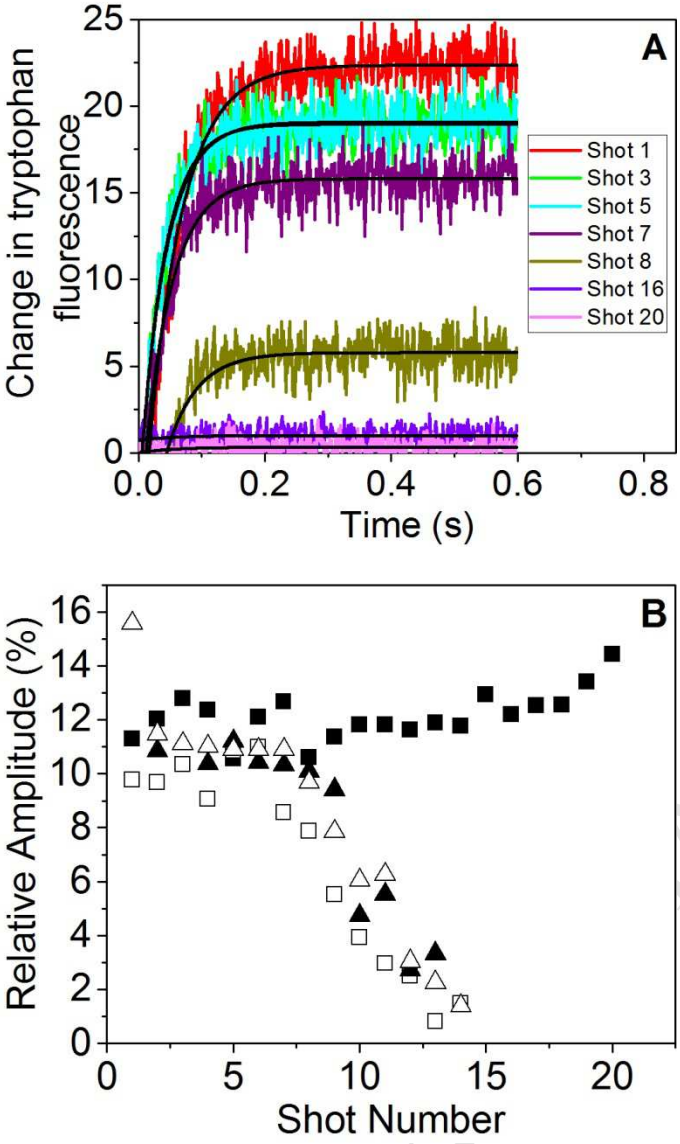

Figure 4: 120 µL 0.5 µM rabbit myosin S1 rapidly mixed with 10 µM ATP. ATP was loaded into the drive syringe as per the standard stopped-flow method while buffer was loaded in the other drive syringe. 120 µL of 1 µM S1 was loaded into the flow circuit via the MVU before 20 'shots' were collected. (A) A selection of transients have been displayed to show that the initial 6-7 transients contain protein and have high amplitudes. After this the protein concentration rapidly decreases as it is replaced with buffer reducing the fluorescence change to zero. (B) The relative fluorescence amplitude for the standard

method (closed squares) versus MVU using a loading volume of 80 µl (open squares), 100 µl (closed triangles) and 120 µl (open triangles).

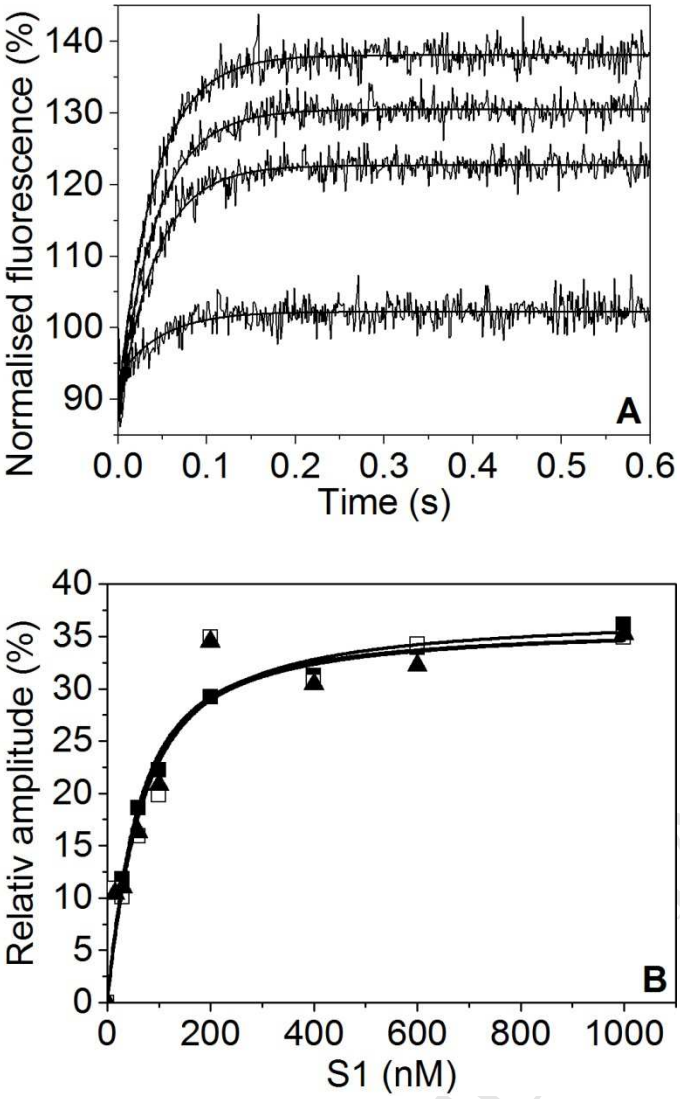

Figure 5: Actin affinity of varied rabbit psoas S1 pre-incubated with 30 nM actin rapidly mixed with 20 µM MgATP using the MVU. The S1 concentration was varied from 0 to 1 µM. (A) Averaged traces from one actin affinity assay. Again each trace was best described by a single exponential which are shown with a solid line. These traces have also been normalised to the start point. (B) Quadratic fit of the relative amplitude versus the S1 concentration. All three repeats have been shown with individual K_D values of 41.7 ± 7.7 nM, 50.5 ± 16.9 nM, and 44.2 ± 13.9 nM. This gave an average K_D value of 45.5 ± 2.6 nM which is in agreement with Kurzawa et al [11]. All concentrations are again those before mixing.

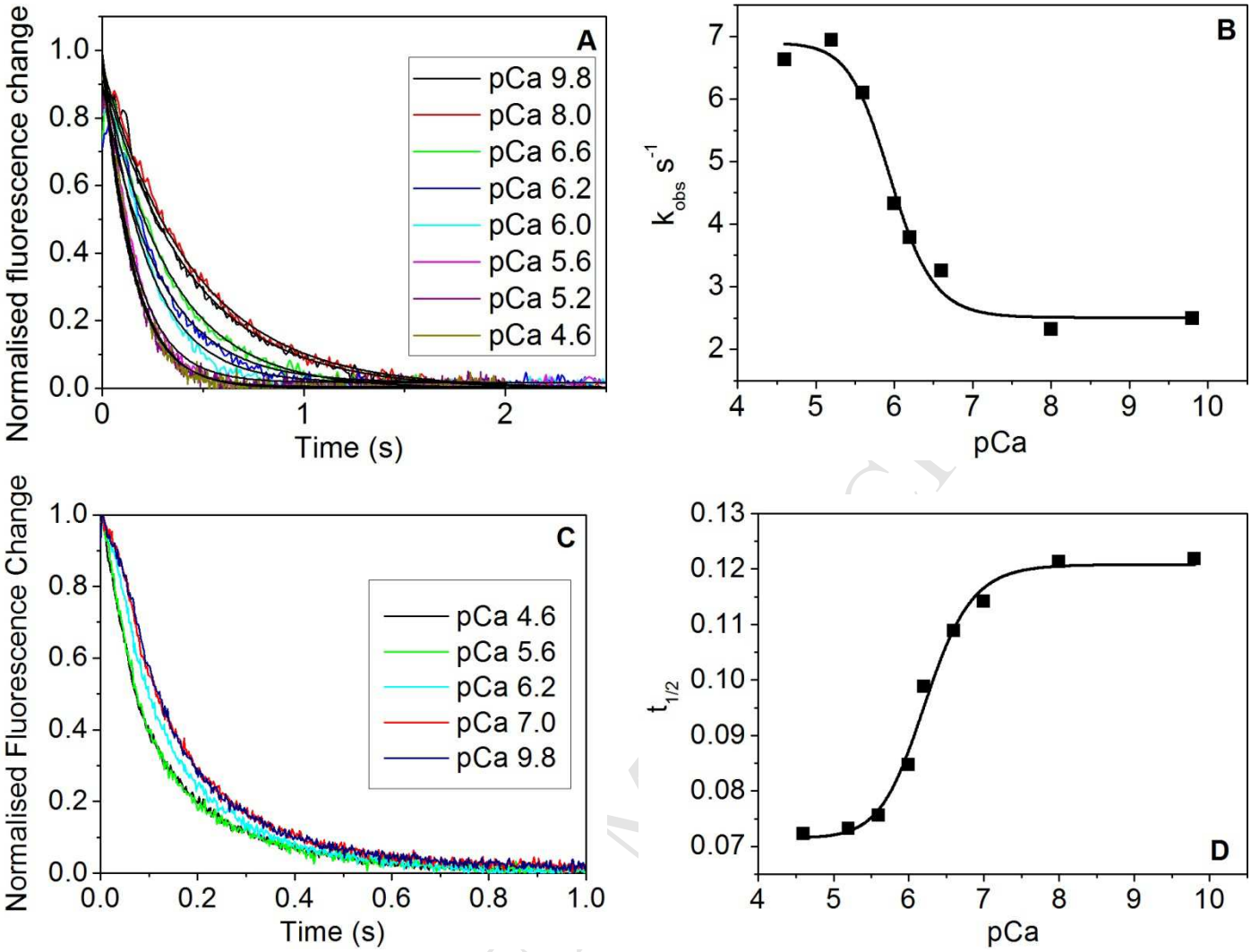

Figure 6: pCa assays using excess actin or excess S1. (A & B) 0.25 µM Rabbit Psoas S1 was rapidly mixed with 10-fold excess pyrene-labelled actin incubated with 2.5 µM skeletal control proteins at different calcium concentrations. (A) Averaged traces from a series of pCa concentrations. These were best described by a single exponential which are shown with a solid line. These traces have been normalised to highlight that the rate constant of S1 binding increases at higher calcium concentrations. (B) A Hill coefficient plot of the observed rate constant versus the pCa. This gave a $pCa_{50\%}$ value of 5.95 which is in agreement with the published value of 6.02 [12]. (C & D) 0.25 µM pyrene-labelled actin + 0.25 µM skeletal control proteins were incubated together then rapidly mixed with excess rabbit psoas S1 (2.5 µM) at different calcium concentrations. (C) Averaged traces

from a series of pCa concentrations. The traces have been normalised to highlight that there is a change in the half-time as the calcium concentration increases. (D) A Hill coeffient plot of the $t_{1/2}$ which is determined as the time at 50% fluorescence. This plot results in a $pCa_{50\%}$ of 6.2 which again is close to the published value of 6.02 [12]. All concentrations are those before mixing.

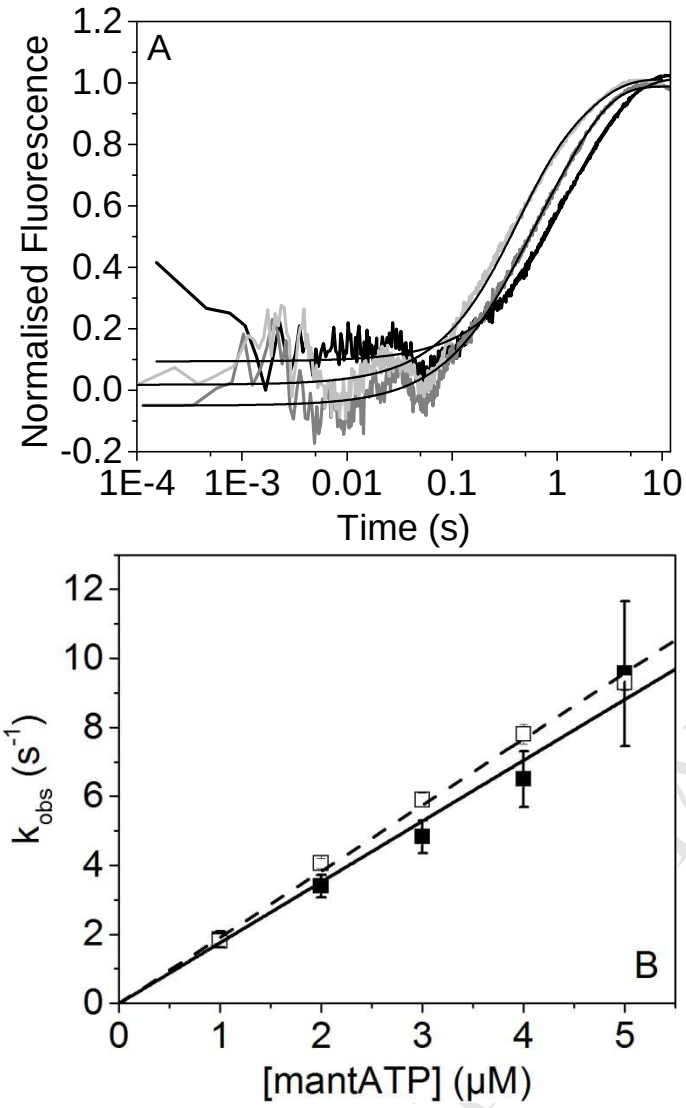

Figure 7: 200 nM Mouse *Gastrocnemius* Myofibrils were rapidly mixed with varying concentrations of mantATP. (A) Average traces obtained by mixing myofibrils with varied mantATP concentrations (1-5 μM) using the MVM. These were best described by a double exponential fit. The traces shown are 2 μM (black line), 3 μM (dark grey line), and 4 μM (light grey line) mantATP. These traces have been normalised to highlight that there is an increase in k_{obs} as the mantATP concentration increases. (B) A linear regression plot of the k_{obs} at mantATP concentrations 1-5 μM. The standard stopped-flow set-up gave a K_1k_{+2} = 1.76 ± 0.07 μM^{-1} s^{-1} while the micro-volume unit set-up gave a K_1k_{+2} = 1.92 ± 0.03 μM^{-1} s^{-1}. Error bars are standard error of the mean. All concentrations are those after mixing.

Assay	Stopped-flow setup	S1 (µg)	Actin (µg)	Tropomyosin (µg)	Troponin (µg)	Myofibrils (Myosin content) (µg)
Actin affinity	Standard	138.3	5	-	-	-
	MVU	33.2	1.2	-	-	-
pCa - Excess Actin	Standard	115	420	187.4	198.8	-
	MVU	27.6	100.8	45	47.7	-
pCa - Excess S1	Standard	1150	42	18.7	19.88	-
	MVU	276	10	4.5	4.77	-
mantATP binding to myofibrils	Standard	-	-	-	-	1123
	MVU	-	-	-	-	269

Table 1: Total mass of protein needed to complete assays illustrated in Figs 4-6 using and the MVU.

Highlights:

- Reduced the volume of sample required in stopped flow systems by a factor of 4
- Many assays using muscle proteins can be completed with <100 µg of protein
- This is the quantity of protein available from <100 mg of muscle tissues
- This will allows assays of human muscle proteins from biopsy tissue